IEEE Access
Multidisciplinary ⋮ Rapid Review ⋮ Open Access Journal

Received 5 June 2024, accepted 4 July 2024, date of publication 10 July 2024, date of current version 19 July 2024.

Digital Object Identifier 10.1109/ACCESS.2024.3426039

RESEARCH ARTICLE

Performance Evaluation of Discrete Wavelet Transform and Machine Learning Based Techniques for Classifying Power Quality Disturbances

UVESH SIPAI[1], (Member, IEEE), RAJENDRASINH JADEJA[1], (Senior Member, IEEE), NISHANT KOTHARI[1], (Member, IEEE), TAPANKUMAR TRIVEDI[1], (Senior Member, IEEE), RAJESH MAHADEVA[2,3], (Member, IEEE), AND SHASHIKANT P. PATOLE[3], (Member, IEEE)

[1]Department of Electrical Engineering, Marwadi University, Rajkot, Gujarat 360003, India
[2]Department of Computer Science and Engineering, Manipal Institute of Technology, Manipal Academy of Higher Education, Manipal 576104, India
[3]Department of Physics, Khalifa University of Science and Technology, Abu Dhabi, United Arab Emirates

Corresponding authors: Shashikant P. Patole (Shashikant.patole@ku.ac.ae) and Rajesh Mahadeva (rajeshmahadeva15@gmail.com)

ABSTRACT This paper evaluates the performance of six different machine learning (ML) algorithms for classifying power quality disturbances (PQDs), with statistical features extracted using discrete wavelet transform (DWT) as feature input. The statistical features have been extracted from coefficients of multi-resolution analysis (MRA) using four different mother wavelets: Daubechies 4 (‘db4’), ‘haar’, Discrete Meyer (‘dmey’), Coiflets 4 (‘coif4’). The performance analysis has been carried out with 5,500 synthetic signals pertaining to eleven different PQDs generated in accordance with IEEE 1159-2019. Moreover, the performance of the classifiers trained with synthetic signals has been investigated under the influence of unseen noisy signals, hardware PQD signals obtained from the experimental setup, and real PQD events. The analysis indicates that the performance of the extra tree (ET) classifier with the features extracted using ‘haar’ as a mother wavelet is superior and robust in comparison to other classifiers, viz k-nearest neighbor (kNN), random forest (RF), decision tree (DT), logistic regression model (LRM), and gaussian naïve bayes (GNB) with features extracted using different mother wavelets. Furthermore, the ‘haar-ET’ based technique demonstrated remarkable performance in classifying PQDs, showing strong generalization to both unseen hardware and noisy signals, and achieving consistent results when tested with real PQD events.

INDEX TERMS Power quality disturbances, discrete wavelet transform, machine learning, classification, extra tree, random forest.

I. INTRODUCTION

Due to the grid integration of renewable energy sources, sophisticated control systems, and rising electricity demand, the modern electrical grid is going through a significant transformation. These developments herald a more complex and challenging era, promising a more efficient and sustainable energy landscape. The increasing incidence of PQDs is one urgent issue that has drawn much attention. PQDs have become more frequent and complex as the grid adapts to accommodate a variety of energy resources, posing a severe threat to the stability and reliability of the power supply [1], [2], [3].

PQDs pose a variety of complex problems. Voltage fluctuations, frequency deviations, waveform distortions, and other anomalies brought on by PQDs can potentially impair the regular operation of electrical machinery and delicate electronic devices. These adversities can result in operational inefficiencies, equipment damage, expensive downtime, and jeopardized safety in crucial applications. PQDs can also

The associate editor coordinating the review of this manuscript and approving it for publication was Ahmed A. Zaki Diab.

increase energy losses, trigger erroneous alarms in protection systems, and affect the integration of renewable energy sources.

Voltage sags and swells brought on by grid faults or unexpected changes in load, are among the most frequent PQDs. Waveform distortion caused by harmonics, is a common PQD that superimposes higher-order frequencies on the fundamental frequency of the power supply. Transients are sudden, temporary deviations from the expected voltage and current waveforms, such as impulsive and oscillatory disturbances. Lighting systems are frequently affected by flicker, which is characterized by noticeable variations in light output and may be brought on by load fluctuations [4].

The aforementioned PQDs are distinct, have different adverse effects on the load or grid [5]. In order to accurately identify and minimize the adverse effects of these disturbances, it is necessary to develop quick and accurate PQDs detection and classification technique [6].

PQDs are typically categorized using a two-step process. Initially, the important characteristics or features are extracted using complex analysis with the help of various signal processing. Then, second step involves using ML based classifiers to identify and categorize PQDs using the extracted features. For feature extraction, several SPTs have been utilized by researchers, which include Fourier transform (FT), fast Fourier transform (FFT), short-time Fourier transforms (STFT), wavelet transforms (WT), discrete wavelet transforms (DWT), wavelet packet transform (WPT), Stockwell transforms (ST), Hilbert-Huang transform (HT), and Kalman filter (KF). The STFT is an extension of the discrete Fourier transform (DFT). However, it has drawbacks when applied to non-stationary and non-linear signals. The WT, in contrast, overcomes these STFT drawbacks by utilizing variable windows tailored for high and low-frequency components, thereby enhancing the time-frequency resolution. The ST, which combines the discrete WT and STFT, is a very durable tool. The S-transform's retention of phase signal information, integration of frequency-based resolution, and the preservation of the time-frequency representation of signals are some of its key characteristics [7].

Artificial intelligence (AI) based techniques called intelligent classifiers are commonly employed for automated decision-making and categorization [8]. Various AI techniques including artificial neural networks (ANN), probability neural network (PNN), support vector machines (SVM), kNN, DT, RF, fuzzy logic, and extreme learning machines have been used for classifying PQDs. Each technique has unique benefits and drawbacks, making it appropriate for various situations. For instance, while PNNs are resilient to noisy data, ANNs are highly adaptable and excel at pattern recognition. SVMs are efficient at handling high-dimensional data, but they might need a lot of computing power. Although kNN is simple and fast, it may have difficulties with large datasets. DT may create complex trees, which leads to overfitting, particularly handling the noisy data. Though it can be computationally intensive, RF, a well-known ensemble technique built on DT, aims to address the overfitting problem by aggregating multiple trees, improving generalization and robustness [9]. The specific PQ disturbance classification requirements, dataset characteristics, and the available computational resources should all be taken into account when choosing a technique, along with the trade-offs between accuracy, interpretability, and efficiency.

A brief review on various signal processing and ML based PQDs classification techniques is presented below. A DWT and PNN based PQDs classification technique has utilized 'db4' as a mother wavelet for feature extraction and artificial bee colony algorithm for optimal feature selection [10]. The performance of the suggested technique is highly sensitive to the higher noise levels. Authors in [11] have demonstrated the distinctness of features extracted using DWT with 'db4'as mother wavelet. The authors have considered real-time PQDs emerging due to converter operation, capacitor switching, and transformer energization. However, the classification of PQDs has not been carried out using the extracted features. The wavelet packet transform was applied in [12] to obtain features from PQD events and given as input to SVM for classification. Dual multiclass support vector machines (MSVM) and tunable-Q wavelet transform (TQWT) are combined to detect and classify PQDs [13], showcasing the advantages of TQWT's capacity to isolate low-frequency interharmonics and extract pertinent features for precise classification. In [14], statistical features were extracted using the DWT with level-6 decomposition and the 'db6' mother wavelet. The non-dominated sorting genetic algorithm II (NSGA-II) is then used for choosing the optimal features given to ANN for classification. A combined discrete gabor transform (DGT) and type-2 fuzzy kernel-based SVM, method for identifying PQDs is presented in [15]. The technique for obtaining and selecting the best feature based on the empirical wavelet transform (EWT) was introduced in [16], where authors highlighted the performance superiority of SVM over other classifiers with the selected features. A hybrid algorithm using ST and HT with DT for the identification and classification of PQDs, have demonstrated its effectiveness, particularly with noisy signals [17]. A novel k-means-based apriori algorithm is implemented in [18] for classifying PQD in a three-phase system. However, only five PQDs classes were considered for the study. The application of dual feed-forward neural network (FFNN) for classifying single and combined PQDs utilizing a novel EWT based adaptive filtering technique is presented in [19]. Authors in [20] have reported the capabilities of convolutional neural network (CNN) for classifying the PQDs. The method combines 1D and 2D CNN architectures and the performance is consistent while maintaining a similar level of computational complexity. Recently, a deep learning neural network based technique is presented in [21] for classifying real PQDs in grid pertaining to four classes. A multidimensional feature-driven ensemble model presented in [22] utilizes time domain, frequency domain and temporal features extracted using bidirectional gated recurrent unit (BiGRU) and fully convolutional networks (FCNs).

For efficient and reliable performance, the ML classifier requires unique features that distinctly characterized different PQDs. In the literature, DWT has been extensively utilised to extract relevant features for PQDs classification. This is due to its MRA capability, which enables the representation of both high and low-frequency components in power quality signals, essential for capturing the variety of disturbance characteristics. The time-frequency localization of DWT allows for effective feature extraction while preserving critical temporal and spectral information. Therefore, the proposed work utilizes DWT for the feature extraction from PQDs. The challenges associated with DWT are the choice of an appropriate mother wavelet and the level of decomposition. Therefore, careful selection is required to ensure unique and reliable feature representation.

Many of the existing techniques for classifying PQDs have not considered various important factors for the study. Such techniques rely on synthetic or simulated data, which might not accurately reflect the complexity of PQDs in the real world [14], [23], [24]. Additionally, some techniques call for complex pre-processing steps or manual feature engineering, which limits their scalability and make them inaccurate [25], [26]. Moreover, instead of a single classifier [10], [18], [27], the performance of multiple classifiers needs to be evaluated with the extracted features to identify the best-suited model for classifying diverse PQDs. Considering the shortcomings of the aforementioned methods, the proposed study aims to develop an accurate and robust PQDs classification technique having superior generalized capabilities. In the proposed work, various mixed-order statistical features have been extracted using DWT for classifying eleven different types of PQDs. The performance evaluation of six different ML algorithms with features extracted using four mother wavelets has been carried out.

The key contributions of this paper are as follows:

- Statistical features extraction from the wavelet coefficients with four different mother wavelets: 'db4', 'haar', 'dmey', and 'coif4' have been used to ensure comprehensive feature representation.
- Four different datasets were used for the performance evaluation: synthetic signals, unseen noisy signals, hardware signals captured using an experimental setup, and real PQD event signals.
- The performance evaluation of kNN, LRM, DT, RF, ET, and GNB classifiers with the proposed statistical features to classify eleven different types of single and multiple PQDs is carried out.
- The robustness, adaptability, and generalized capabilities of the model is demonstrated by assessing its performance with unseen noisy signals, hardware signals, and real PQD event signals, despite being trained on noiseless synthetic signals.

The rest of the paper is structured as follows: Section II describes the methodology, the proposed method is discussed in Section III, Section IV presents the results and discussion, and the conclusion is drawn in section V.

II. METHODOLOGY

The methodology is divided into two main parts: DWT and MRA, and ML Classifiers. The following subsections provide a comprehensive overview of these techniques and approaches.

A. DWT AND MRA

The wavelet transform is an effective tool for identifying and categorizing power quality disturbances as it can handle non-stationary signals [28]. The WT functions across the frequency and time domains by employing an adjustable wavelet (ψ), as demonstrated by its ability to analyze signals in both domains [29]. Following is a mathematical equation of temporal-frequency plane [30],

$$\gamma(s,\tau) = \int x(t)\,\psi^{*}_{s,\tau}(t)\,dt,\ \psi_{s,\tau}(t) = \frac{1}{\sqrt{s}}\psi\left(\frac{t-\tau}{s}\right) \tag{1}$$

where (s,τ): a scale – translation plane, and $x(t)$: the signal analyzed. It should be noted that performing WT needs substantial calculations because it must be done at every location along the $s-\tau$ plane. The mother wavelet (ψ) is squeezed to test over different levels. DWT is an effective variant of WT where the parameter 'γ' in eq. (1) is computed at select locations within the $s-\tau$ plane.

In this context, the $s-\tau$ plane is discretely sampled using a dyadic grid, similar to MRA principles, where $s = 2^j$ and $\tau = 2^j k$, with j and k being integers. To handle the lower frequency spectrum in MRA, the second function called the scaling function (Φ) is used in addition to wavelet (Ψ). These functions, when employing dyadic sampling, are defined by the following equation [4]:

$$\psi_{j,k}(t) = 2^{-(j/2)}\psi(2^{-j}t-k) \tag{2}$$
$$\phi_{j,k}(t) = 2^{-(j/2)}\phi(2^{-j}t-k) \tag{3}$$

In practical terms, the implementation of DWT resembles a strategy akin to 'sub-band coding'. This involves breaking down a signal iteratively into different scales or levels using a filter bank. Within each scale or level, the signal undergoes filtration utilizing a combination of high-pass (g) and low-pass (h) filters, resulting in outputs categorized as "detail" and "approximation", respectively. At each level, the signal undergoes down-sampling by a factor of "2", and the approximation component is selected for subsequent decomposition. The recursive equations that govern the detail $d_j(k)$ and approximation $a_j(k)$ components of the j^{th} level are as follows:

$$d_j(k) = \sum\nolimits_n g(n)a_{j+1}(2k+n) \tag{4}$$
$$a_j(k) = \sum\nolimits_n h(n)a_{j+1}(2k+n) \tag{5}$$

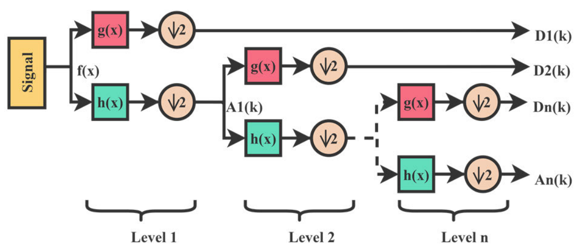

FIGURE 1. Decomposition of signal using DWT up to n^{th} level.

Fig. 1 represents the MRA of the time domain signals using DWT up to the n^{th} level of decomposition. The signal passes through a set of high-pass and low-pass filters at each stage to provide the detail and approximate coefficient of each level. These coefficients can also be used to obtain relevant details for further investigation.

B. CLASSIFIERS

The fundamental classification task in ML is to categorize an input data point into one of many predefined categories or classes. This process involves discovering patterns and relationships within the data, allowing the model to predict or take action regarding unforeseen circumstances reliably. Automating this classification process with the help of ML algorithms opens up various possibilities, including the detection of PQDs. The classification algorithms considered in this study are briefly presented below.

1) kNN

Due to its adaptability and accessibility of use, the kNN algorithm is a popular ML method. Since kNN does not make any assumptions about the data distribution, it may be used for tasks like regression and classification on a variety of datasets that contain both numerical and categorical characteristics. kNN offers flexibility since it is a non-parametric approach that doesn't rely on preconceived notions about the underlying data structure. One feature that distinguishes it from other algorithms is its resilience to outliers [31].

This algorithm determines Euclidean distance between k neighbors that are closest to a given data point. A majority vote or an average procedure is then used to determine the class or value of the data item [32].

2) LRM

A linear model called LRM is employed in categorization. It makes use of the logistic function to calculate the likelihood that an instance belongs to a specific class [33]. By nature, LRM is a binary classification technique that estimates the likelihood that an instance falls into a certain class. On the other hand, it may be expanded to address multiclass classification issues by utilizing methodologies such as one-versus-one (OvO) or one-versus-rest (OvR) [34].

3) DT

Encapsulating a sequence of decisions and their possible results, a DT is a hierarchical, tree-like structure. Every node within the tree serves as a point where a decision is made, and the branches extending from it illustrate the potential outcomes that follow. Ultimately, the terminal leaves of the tree encapsulate conclusive decisions or predictions. The tree is built via recursive data partitioning, with core nodes, branches, and leaf nodes representing dataset properties, decision rules, and outcomes, respectively [35]. The DT starts at a root node and grows into branches to build a complete tree-like structure [36].

4) RF

In ML, RF is a potent supervised learning technique that excels at classification and regression tasks. It builds an ensemble of DT trained on different subsets of the dataset and uses their average predictions as a meta-estimator to improve overall accuracy and reduce overfitting. Using the bagging approach, which involves training each DT on a subsample taken with replacement from the original dataset, this "forest" of DT is created. Based on the idea of ensemble learning, the ensemble technique combines predictions from several models to improve model performance and solve complicated issues [37]. The main advantage of RF is in its capacity to build a variety of DTs and aggregate their results via majority vote, producing reliable predictions.

5) ET

An ensemble learning method called the ET classifier is similar to the RF, but differs in how it builds DTs inside the forest. In this approach, every DT is constructed using the whole original training sample, and at every test node, the tree is supplied with a random subset of k characteristics to consider for reaching a choice. Each DT is prompted by this feature subset to choose the optimal feature for the data split separately using a given mathematical criterion, which is the gini index. Several decorrelated DT are produced by using a random sample of features, which increases the variety of the ensemble [38].

The classification process of ET classifier is as follows: suppose X represents the input feature matrix of size $l \times m$, where l is the number of samples and m is the total number of features. Every column denotes a feature, and every row, x_i, indicates a sample. Let z be the corresponding target vector of size $p \times 1$ for classification. Given a set of decision trees $T = \{T_1, T_2, T_3, \ldots T_M, \}$, the prediction of the ET classifier is given by:

$$\hat{z_i} = mode\left(T_1\left(x_i\right), T_2\left(x_i\right), T_3\left(x_i\right), \ldots T_M\left(x_i\right)\right) \quad (6)$$

where $\widehat{z_i}$ is the predicted output for sample x_i and M denotes the number of trees in the ensemble.

ET, in particular, presents a novel feature selection procedure for building forests. It determines the normalized overall decrease in the selected mathematical criterion by computing the gini importance for every feature. This enables users to choose features by arranging them according to their gini importance in descending order and then choosing the top k features according to their preferences. ET, in contrast to RF, uses random sampling for every tree without replacement, producing distinct datasets for a variety of decision tree training scenarios. Its unique quality also resides in the random feature splitting value selection, which helps to generate diverse and uncorrelated DTs in the ensemble [32].

To the best of our knowledge, the application of ET classifier has not been reported in the literature for classifying PQDs.

6) GNB

Based on Bayes' theorem, the GNB method is an effective tool for handling classification issues, especially when dealing with high-dimensional datasets like text categorization. GNB is well-known for being straightforward and efficient. It can build ML models fast enough to generate predictions. GNB is a probabilistic classifier that uses characteristics to determine probability of an object. It is used in several fields, such as article classification, spam filtering, and analyzing sentiment. It applies the Bayes theorem to handle categorization problems utilizing past information to compute a probability of hypothesis and uses that result as the foundation for its decision-making [32]. Being a probabilistic classifier, it predicts based on the probability of an item.

III. PROPOSED TECHNIQUE

Fig. 2 illustrates the flow chart of the proposed method for identifying and classifying PQDs. Additionally, a concise explanation of each step is presented in the following subsections.

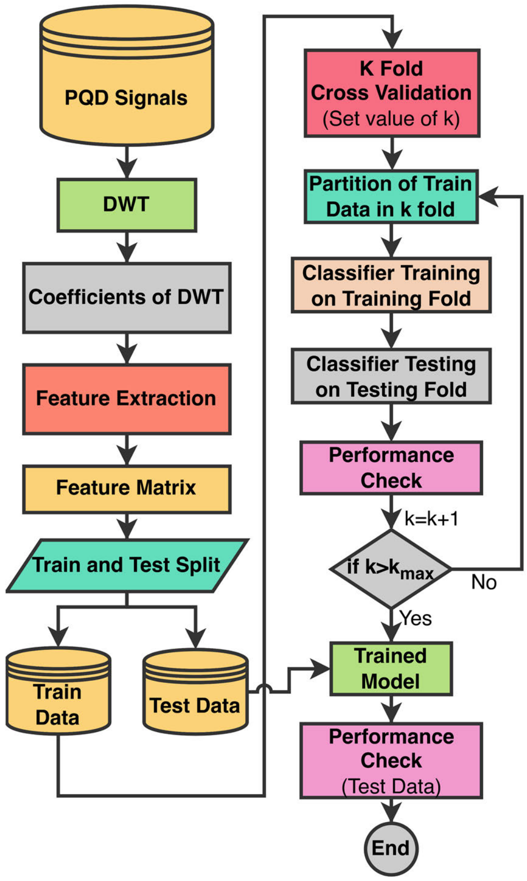

FIGURE 2. Flow chart of the proposed method for PQDs classification.

A. PQDs DATA COLLECTION

It is quite challenging to acquire all real-time PQD event signals from the electrical network for categorization research. Therefore, in the proposed work, various PQD signals have been generated using the numerical models as mentioned in Table 1 [39]. It is essential that all generated PQD signals strictly comply with definitions of IEEE 1159 [40]. This is to ensure the validity and applicability of the research by closely simulating actual PQD events in the electrical network. In the presented work, all the PQD signals' parameters have been varied in accordance with IEEE 1159-2019.

In the proposed study, eleven distinct types of PQD signals have been generated using MATLAB. Each type of signal denoted as a separate class includes CL1: normal, CL2: sag, CL3: swell, CL4: interruption, CL5: impulsive transient, CL6: oscillatory transient, CL7: harmonics, CL8: flicker, CL9: notch, CL10: harmonics with sag, and CL11: harmonics with swell. To ensure a balanced dataset, a total of 5,500 signals have been generated, with 500 unique signals corresponding to each of the eleven classes. Special care has been taken to ensure that each signal is unique within its respective class. The normalized amplitude has been set to 1 per unit, and the fundamental frequency is fixed at 50 Hz. Each signal has a 10-cycle length with 100 samples per cycle at a 5 kHz sampling frequency. Fig. 3 represents the waveforms of PQDs for CL2 to CL11. The aforementioned dataset is publicly shared on IEEE Dataport and Harvard Dataverse, which provide accessible platforms for researchers to access, analyze, and contribute to PQD research [41], [42].

Apart from simulated signals, a total of 330 PQDs pertaining to eleven classes have been recorded using an experimental setup in the laboratory. Furthermore, recorded real PQD events data available on the IEEE Dataport [43], [44] has been utilized to validate the performance of the proposed approach. The detailed description of the hardware and real PQD event data is discussed in section IV.

The simulation of PQD signals that accurately reflect the complexity and variety of actual disturbances that occur within power grids is made possible by the meticulous variation in the generated data.

B. FEATURE EXTRACTION

In the proposed work, feature extraction has been accomplished using a two-stage process. Firstly, wavelet coefficients have been extracted using DWT-MRA analysis. Secondly, various statistical features have been obtained from the wavelet coefficients. The detailed process is described below.

TABLE 1. Numerical model equations of PQDs.

PQDs	Numerical Model Equations	Parameters
CL1: Normal	$y(t) = M\,sin(wt)$	$w = 2\pi f$ $0.9 \leqslant M \leqslant 0.1$
CL2: Sag	$y(t) = M\left[1 - \alpha\left(u(t - t_x) - u(t - t_y)\right)\right] sin(2\pi f t)$	$0.1 \leqslant \alpha \leqslant 0.9$ $T \leqslant t_y - t_x \leqslant 9T$
CL3: Swell	$y(t) = M\left[1 + \alpha\left(u(t - t_x) - u(t - t_y)\right)\right] sin(2\pi f t)$	$0.1 \leqslant \alpha \leqslant 0.8$ $T \leqslant t_y - t_x \leqslant 9T$
CL4: Interruption	$y(t) = M\left[1 - \alpha\left(u(t - t_x) - u(t - t_y)\right)\right] sin(2\pi f t)$	$0.9 \leqslant \alpha \leqslant 1$ $T \leqslant t_y - t_x \leqslant 9T$
CL5: Impulsive Transient	$y(t) = M[1 - \alpha_i\{u(t - t_x) - u(t - t_y)\}]\, sin(2\pi f t)$	$0 \leqslant \alpha_i \leqslant 0.414$ $T/20 \leqslant t_y - t_x \leqslant T/10$
CL6: Oscillatory Transient	$y(t) = M\left[sin(2\pi f t) + \alpha^{-c(t - t_x)/\tau} \sin w_n\,(t - t_x) u(t_y) - u(t_x)\right]$	$0.1 \leqslant \alpha \leqslant 0.8$ $0.5T \leqslant t_y - t_x \leqslant 3T;\ 8_{\text{ ms}} \leqslant \tau \leqslant 40_{\text{ ms}}$ $300 \leqslant f_n \leqslant 900_{\text{ Hz}}$
CL7: Harmonics	$y(t) = M[\alpha_1 sin(2\pi f t) + \alpha_3 sin(3 * 2\pi f t) + \alpha_5 sin(5 * 2\pi f t)$ $+ \alpha_7 sin(7 * 2\pi f t)]$	$0.05 \leqslant \alpha_3, \alpha_5, \alpha_7 \leqslant 0.15$ $\sum \alpha_i^2 = 1$
CL8: Flicker	$y(t) = M\left[1 + \alpha_f\, sin(\beta w t)\right] sin(2\pi f t)$	$0.1 \leqslant \alpha_f \leqslant 0.25$ $8 \leqslant \beta \leqslant 20\ Hz$
CL9: Notch	$y(t) = M\,sin(2\pi f t) - sign(sin(2\pi f t))$ $\times \left\{\sum_{n=0}^{9} \kappa \left[u(t - (t_x - 0.02n)) - u\left(t - (t_y - 0.02n)\right)\right]\right\}$	$0 \leqslant t_y t_x \leqslant 0.5T$ $0.01T \leqslant t_y - t_x \leqslant 0.05T$ $0.1 \leqslant K \leqslant 0.4$
CL10: Harmonics with Sag	$y(t) = M\left[1 - \alpha\left(u(t - t_x) - u(t - t_y)\right)\right] [\alpha_1 sin(2\pi f t)$ $+ \alpha_3 sin(3 * 2\pi f t) + \alpha_5 sin(5 * 2\pi f t)]$	$0.1 \leqslant \alpha \leqslant 0.9$ $0.05 \leqslant \alpha_3, \alpha_5, \alpha_7 \leqslant 0.15$ $T \leqslant t_y - t_x \leqslant 9T$
CL11: Harmonics with Swell	$y(t) = M\left[1 + \alpha\left(u(t - t_x) - u(t - t_y)\right)\right] [\alpha_1 sin(2\pi f t)$ $+ \alpha_3 sin(3 * 2\pi f t) + \alpha_5 sin(5 * 2\pi f t)]$	$0.1 \leqslant \alpha \leqslant 0.8$ $0.05 \leqslant \alpha_3, \alpha_5, \alpha_7 \leqslant 0.15$ $T \leqslant t_y - t_x \leqslant 9T$

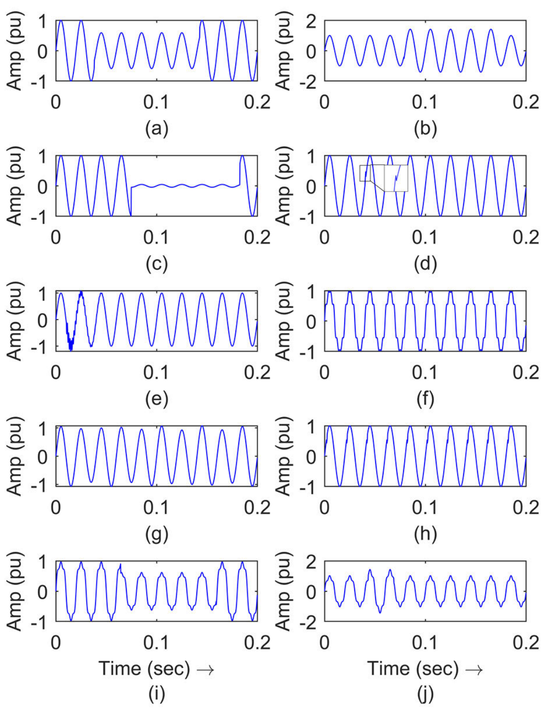

FIGURE 3. PQDs Waveforms: (a)Sag, (b)Swell, (c)Interruption, (d)Impulsive Transient, (e)Oscillatory Transient, (f)Harmonics, (g)Flicker, (h)Notch, (i)Harmonics with Sag, and (j)Harmonics with Swell.

1) DWT-MRA

In the proposed work, DWT has been used to extract relevant information from various PQDs signals. A crucial step in extracting features from raw signals is choosing the mother wavelet. The proposed research has chosen four different mother wavelets – 'db4', 'haar', 'dmey', and 'coif4'. These mother wavelets are popular and find wide applications because of their unique characteristics and suitability for capturing various features in PQD signals. The 'haar' wavelet is valued for detecting sudden disturbances due to its usefulness in revealing abrupt signal changes and simplicity. The 'db4' is preferred for its balanced representation of oscillatory and transient components. The 'dmey' wavelet is chosen because of its capabilities to capture granular signal details at various scales. The 'coif4' wavelet is effective in analyzing signals with smooth variations, and it has the capability to provide a good balance between time and frequency localization accurately for both high and low-frequency components in a signal [45].

The PQD signals are subjected to level 4 decomposition using the chosen wavelets for thorough analysis. Four detailed coefficients D1, D2, D3, and D4, and one approximation coefficient A4, corresponding to the final multiresolution decomposition, are extracted. These coefficients form the basis for subsequent feature extraction procedures, making it possible to extract and characterize important information from PQD signals efficiently. Extracted coefficients from the PQD signal using the 'haar' mother wavelet are illustrated in Fig. 4 for CL9: notch disturbance.

2) STATISTICAL FEATURE CALCULATION

The extraction of distinct features from PQD signals is essential for efficient classification and identification tasks. These

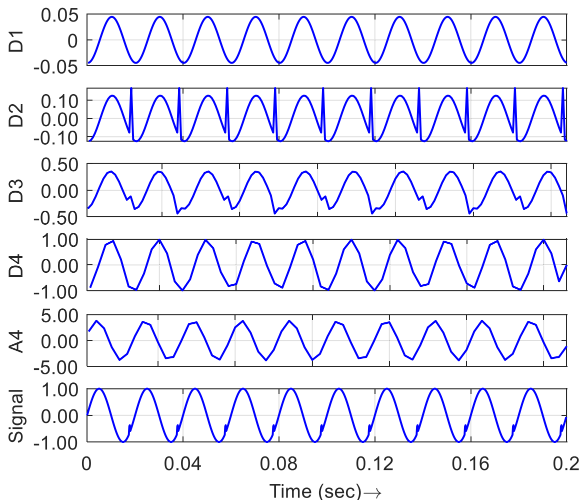

FIGURE 4. Detailed and approximation coefficient extracted using 'haar' mother wavelet for CL9: Notch.

features serve as vital inputs for AI classifiers that help to distinguish between different PQDs. The DWT-derived coefficients have been meticulously analyzed as part of the feature extraction process to extract relevant information from the PQD signals. The statistical features obtained from the aforementioned wavelet coefficients include root mean square (RMS), mean, standard deviation, variance, range, skewness, kurtosis, average deviation, entropy, min, max, and energy as expressed mathematically in Table 2.

The visualization of the features in higher dimensional space is not feasible. A non-linear technique called t-distributed stochastic neighbor embedding (t-SNE) preserves the local patterns and groups of the original high-dimensional data while projecting it into a space with fewer dimensions. This technique is useful for visual inspection because it allows for the investigation of resemblance and relationships between various features [46]. The t-SNE approach is used in the proposed work to aid in the visual representation of complex statistical feature sets derived from various wavelet coefficients. This offers insights into the vividness between the feature spaces generated by the various wavelet families. Fig. 5 shows the t-SNE plot for feature extracted with (a)'db4', (b)'haar', (c)'dmey', and (d)'coif4' as mother wavelets for different eleven PQD classes. The t-SNE plot illustrates the feature distribution across different classes of PQD data, revealing distinct clusters in the two-dimensional space for each class.

C. CLASSIFICATION

The statistical features discussed in the previous subsection have been normalized and given to different ML algorithms for classifying PQDs. The performance of kNN, DT, ET, LRM, RF, and GNB classifiers has been evaluated with the proposed features. Out of a total of 5,500 cases corresponding to eleven PQD classes, 4,400 (80%) cases have been used to train the model. The testing is performed on the remaining 1,100 (20%) cases. The classification has been carried out

TABLE 2. Statistical features.

Feature	*Mathematical Equation*	*Feature*	*Mathematical Equation*
RMS	$\sqrt{\frac{1}{N}\sum_{i}^{N} k_i^2}$	Kurtosis	$\frac{1}{N}\sum_{i}^{N}\left[\frac{(k_i-\mu)}{\sigma}\right]^4$
Mean	$\frac{1}{N}\sum_{i}^{N} k_i$	Average Deviation	$\frac{1}{N}\sum_{i}^{N}\lvert k_i-\mu\rvert$
Standard Deviation	$\sqrt{\frac{\sum_i^N (k_i-\mu)^2}{N}}$	Entropy	$-\sum_{i}^{N} P(k_i)\log P(k_i)$
Variance	$\frac{1}{N}\sum_{i}^{N}(k_i-\mu)^2$	Minimum	$\min(k)$
Range	$\max(k)-\min(k)$	Maximum	$\max(k)$
Skewness	$\frac{1}{N}\sum_{i}^{N}\left[\frac{(k_i-\mu)}{\sigma}\right]^3$	Energy	$\sum_{i}^{N}\lvert k_i\rvert^2$

using the Python 3.10.9 environment with the system having specifications as an Intel® Core^{TM} i7 8th generation CPU, 16GB of RAM, and a 2GB NVIDIA GeForce 940MX graphics processing unit (GPU).

Each classifier requires some hyper-parameter settings for classification. The classier performance is significantly impacted by the choice of the hyper-parameters. In the proposed work, grid search cross-validation (Grid Search CV) technique has been used for hyper-parameter tuning of all the classifiers. Grid Search methodically investigates a variety of hyper-parameters to enhance the performance of the classifier. A five-fold CV is used to tune the parameters during the training of the classifiers. The best hyper-parameters for the classifiers obtained through the Grid Search CV technique in the proposed work are mentioned in Table 3.

The training and testing process is carried out uniformly for all classifiers, enabling a thorough evaluation and comparison of their performance in PQD classification and identification tasks.

IV. RESULTS AND DISCUSSION

The performance of the proposed technique is evaluated with noiseless and noisy synthetic signals, hardware signals obtained from experimental setup, and real PQD events. The performance analysis is presented in the following subsections.

A. PERFORMANCE WITH NOISELESS SIGNALS

In this section, the performance of the classifiers with the noiseless (NL) signal is presented. As described in the previous section, the statistical features extracted from coefficients of MRA of PQD signals considering mother wavelets 'db4', 'haar', 'dmey', and 'coif4' have been used for the

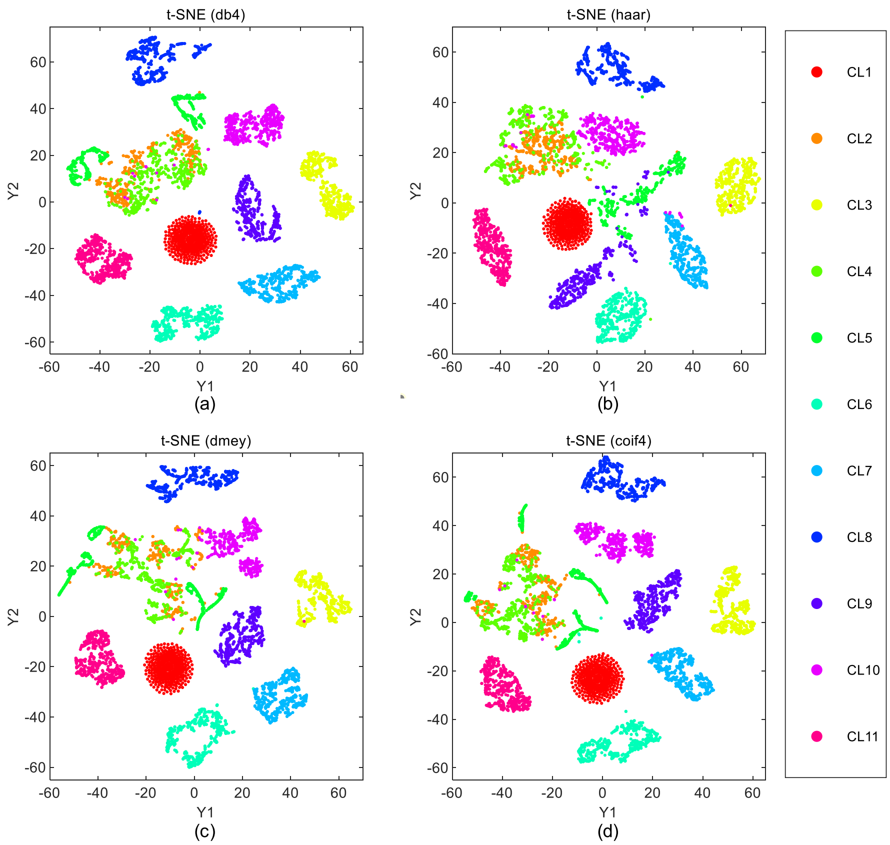

FIGURE 5. t-SNE visualizations of statistical features extracted using (a)db4, (b)haar, (c)dmey, and (d) coif4 mother wavelet for various PQDs.

TABLE 3. Hyper-parameters of the classifiers.

Classifier	*Hyperparameters*
kNN	n_neighbors: 6; weights: 'uniform'; metric: 'minkowski'
LRM	solver: 'lbfgs'; penalty: 'l2'; C: '1'
DT	criterion: 'gini'; max_depth: 'None' min_samples_split: '2'; min_samples_leaf: '1'
RF	max_features: 'sqrt'; n_esti`mators: '100'
ET	max_depth: 'None'; min_samples_split: '2' min_samples_leaf: '1'
GNB	priors: 'none'; var_smoothingfloat: '1e-9'

performance assessment of the classifiers. Six different classifiers have been trained using the extracted features with 80% of the total PQD cases, and the remaining 20% cases have been used for performance evaluation of the trained classifiers.

The performance of classifiers in terms of cross validation (CV) mean score, training and testing accuracy is mentioned in Table 4 for different mother wavelets. From Table 4, it is evident that the kNN performs consistently across all mother wavelets in terms of CV mean scores and testing accuracies, demonstrating robustness to the choice of wavelet transform. Nevertheless, when compared to other classifiers, the performance is poor. The LRM classifier demonstrates excellent generalization by performing consistently and reliably across all mother wavelets with high CV scores. The performance of DT is at par with the kNN, but the testing accuracy varies between wavelet transforms, suggesting its sensitivity to the choice of mother wavelets.

The performance of RF and ET classifiers is consistent and identical for different choices of wavelet. Out of all the classifiers, the performance of GNB is inferior in the PQD classification context, and its CV mean scores and test accuracies are lower than those of other classifiers with the proposed features.

Further, Fig. 6 illustrates the class-wise performance of the classifiers with different mother wavelets. In particular, all the classifiers demonstrate remarkable 100% accuracy for CL1: normal, CL7: harmonics, and CL11: harmonics with swell. Whereas, in classifying CL2: sag and CL4: interruption, the performance of all the classifiers has been sensitive to the choice of mother wavelet except for LRM. The difficulty in discrimination between CL2: sag and CL4: interruption is also evident from the t-SNE plot represented in Fig. 5.

Fig. 7 summarizes the test performance of classifiers with different mother wavelets. It is notable from Table 4 and Fig. 7 that the LRM classifier has identical performance with

TABLE 4. Performance of the classifiers with different mother wavelets with noiseless data.

	'db4'			'haar'			'dmey'			'coif4'		
Classifier	CV Mean score	Training Accuracy	Testing Accuracy	CV Mean score	Training Accuracy	Testing Accuracy	CV Mean score	Training Accuracy	Testing Accuracy	CV Mean score	Training Accuracy	Testing Accuracy
kNN	97.47%	100%	97.36%	97.36%	100%	97.72%	97.59%	100%	97.45%	97.82%	100%	97.64%
LRM	99.52%	99.97%	99.63%	98.06%	98.93%	99%	99.5%	100%	99.72%	99.52%	100%	99.73%
DT	97.50%	100%	97.36%	99.11%	100%	99.36%	97.75%	100%	96.72%	98.52%	100%	98.64%
RF	98.45%	100%	98.54%	99.63%	100%	99.81%	98.70%	100%	98.54%	98.73%	100%	99.18%
ET	98.29%	100%	98.72%	99.75%	100.%	99.81%	98.52%	100%	98.63%	98.64%	100%	98.73%
GNB	97.20%	97.25%	97.27%	96.25%	96.25%	97%	96.02%	96.11%	96.63%	97.02%	97.25%	97.18%

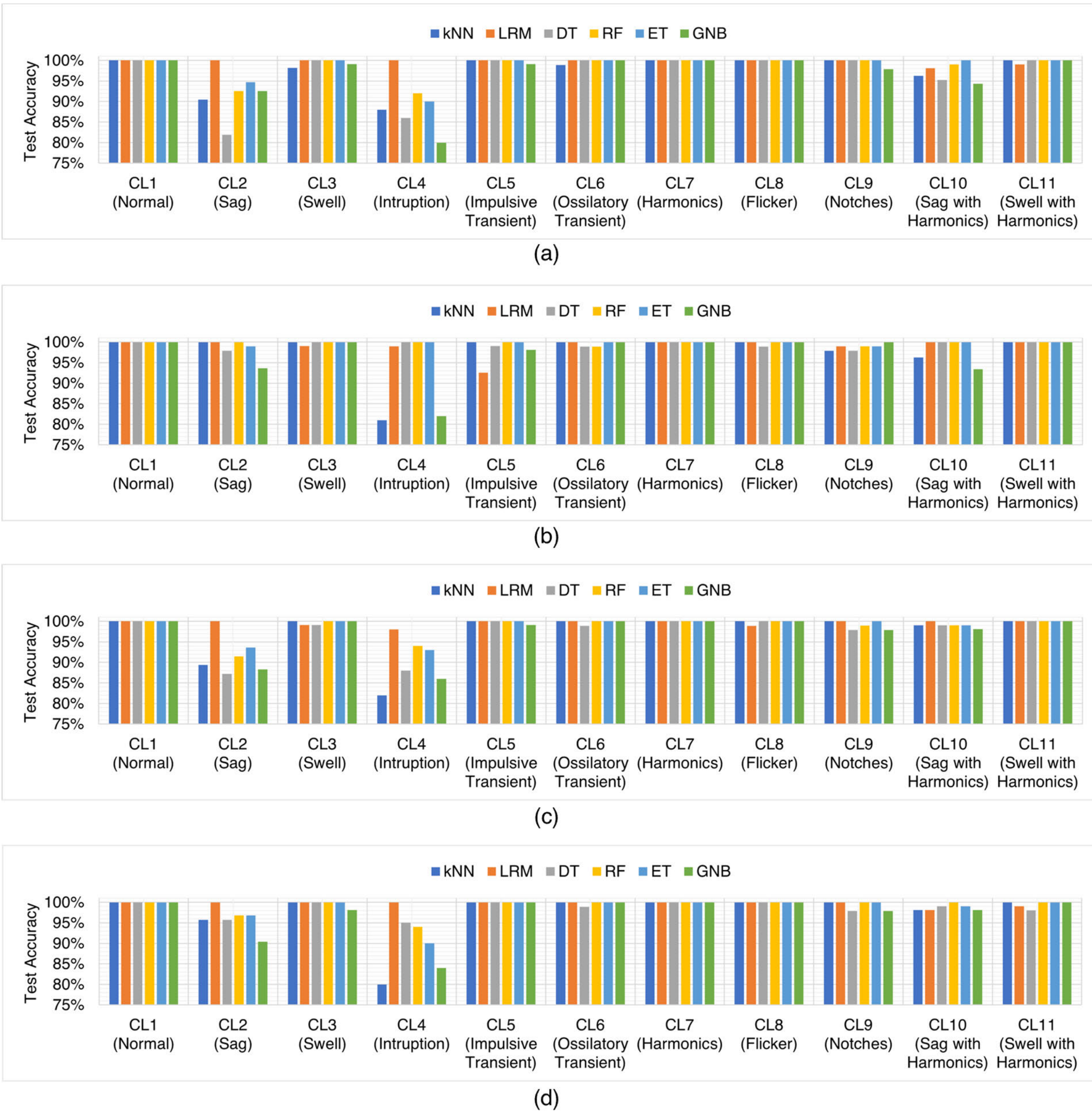

FIGURE 6. Class wise accuracy of the classifiers with feature sets of (a)'db4', (b)'haar, (c)'dmey', and (d)'coif4'.

the features extracted using 'db4', 'dmey', and 'coif4' as the mother wavelet. However, the performance of LRM has been lower in comparison to RF and ET classifiers with the 'haar' mother wavelet.

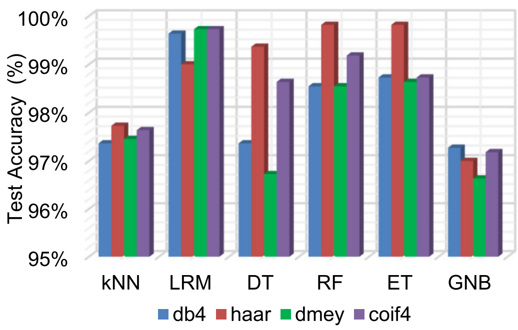

FIGURE 7. Performance of the classifiers with different mother wavelets.

The overall performance of RF and ET classifiers has been consistent in classifying different PQDs with features extracted using ‘haar’ as the mother wavelet with an overall accuracy of 99.81%.

B. PERFORMANCE WITH NOISY SIGNALS

The robustness of the presented method in the presence of noise has been evaluated by introducing noise to the separately generated PQDs. To carry out a thorough evaluation, a set of 1,100 new PQD signals corresponding to eleven classes (100 signals for each class) has been generated. Various levels of white Gaussian noise with signal-to-noise ratio (SNR) of 50 dB, 40 dB, 30 dB, and 20 dB have been deliberately introduced to 10% of the signals in each class randomly. This experimental design provides an essential validation of the classifier’s performance under the uncertainty of noise-induced signals in real-world applications. The statistical features were extracted in a similar manner as discussed previously using four different mother wavelets. The classifier models trained with noise-less signals (described in the previous sub-section) have been tested with newly generated PQDs consisting of random noise signals in each class. Hence, the performance of the classifiers in the presence of random noise signals has been evaluated with a totally unseen dataset. The results of this thorough evaluation have been presented below.

The performance in terms of classification accuracy of the classifiers for classifying PQDs with noise is shown in Fig. 8. It is evident from Fig. 8 that the performance of all the classifiers has significantly declined with an increase in noise level for the features extracted using ‘db4’ and ‘dmey’ mother wavelets. The LRM classifier has shown consistent performance with the ‘coif4’ mother wavelet up to 30 dB SNR; however, at lower SNR (20 dB), the performance has significantly declined.

The performance of the classifiers is less susceptible to noise when features are extracted using the ‘haar’ mother wavelet. Overall, ET and RF outperformed other classifiers with features extracted using the ‘haar’ mother wavelet for different noise levels in the signals. The classifier’s performance in the presence of noise signals is in concurrence with the performance under noise-less signals.

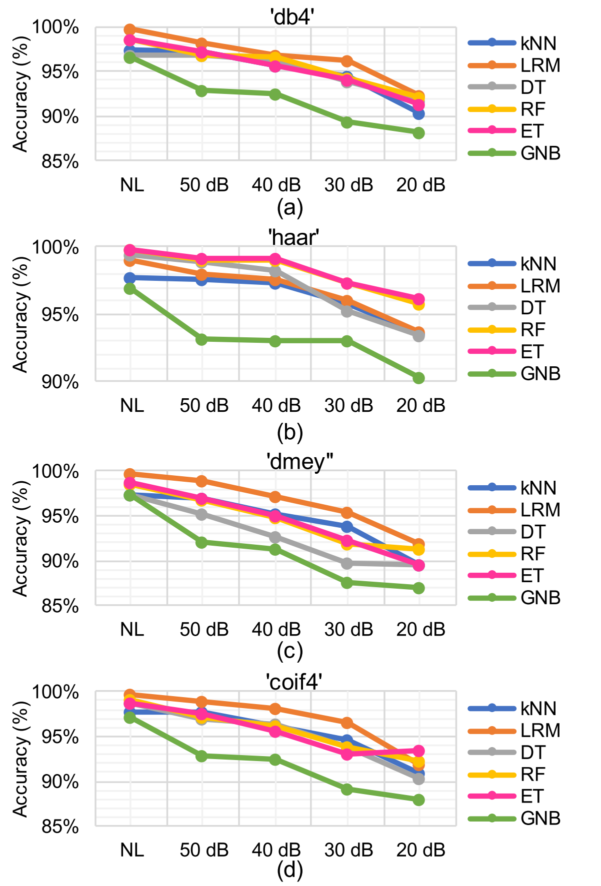

FIGURE 8. Performance of classifiers with feature extracted using (a) ‘db4’, (b) ‘haar’, (c) ‘dmey’, and (d)’coif4’ mother wavelet under noisy condition.

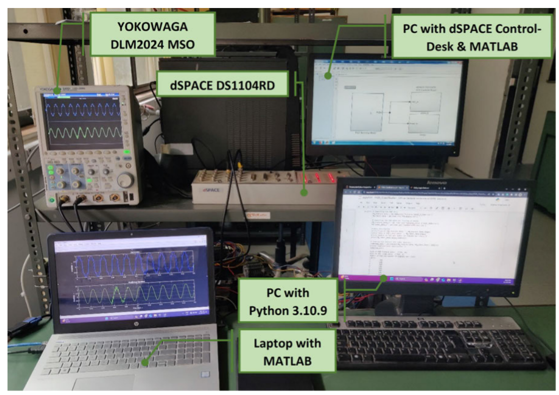

FIGURE 9. Experimental setup to generate PQDs.

The above discussion demonstrates that selecting the mother wavelet is crucial in PQD classification. The performance of the classifiers is highly sensitive to the choice of mother wavelet while classifying PQDs in the presence of noise.

C. PERFORMANCE WITH HARDWARE SIGNALS

The efficacy of the proposed method has been tested for PQD signals obtained from hardware set up in the laboratory. Fig. 9

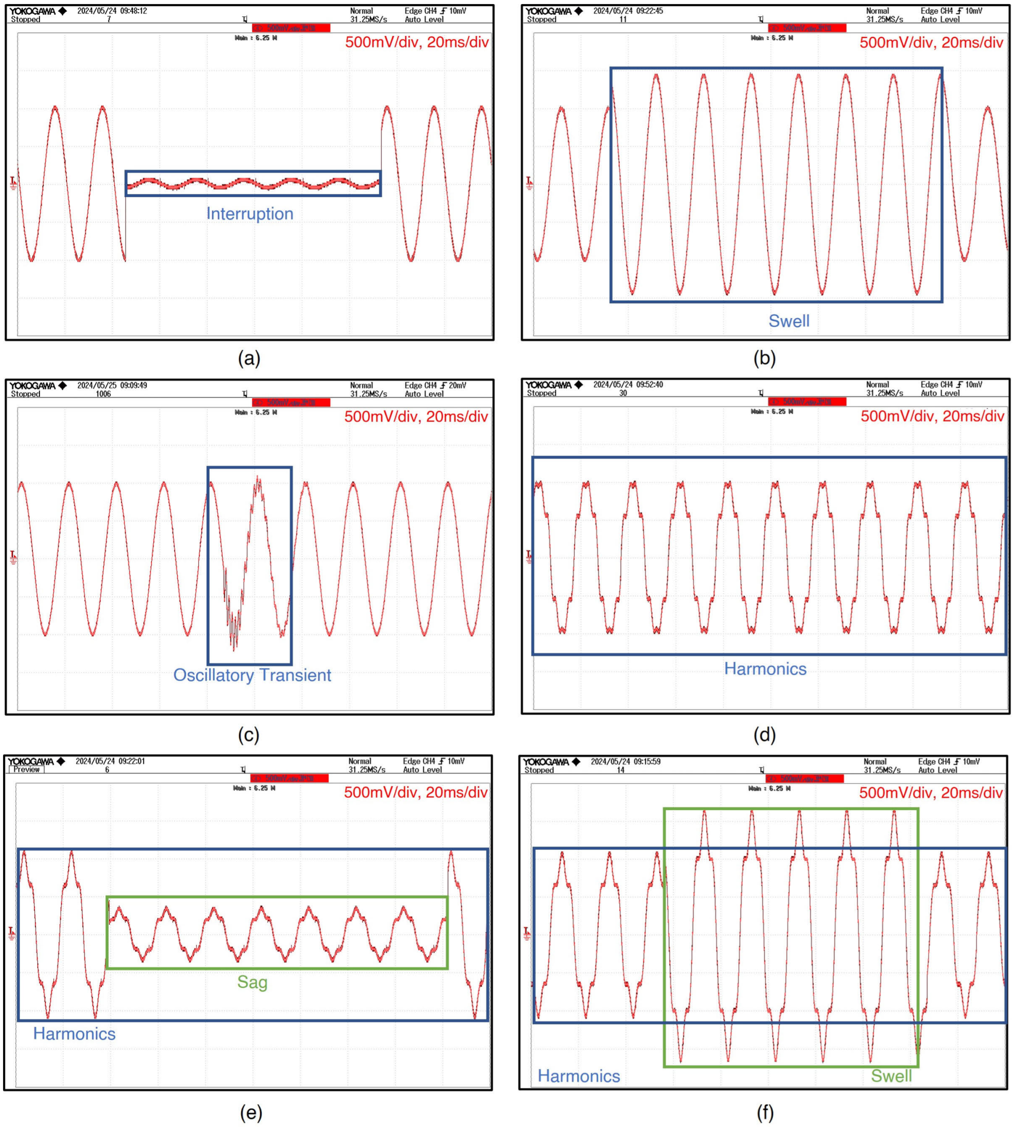

FIGURE 10. The signal generated using experimental setup (a)interruption, (b)swell, (c)oscillatory transient, (d)harmonics, (e)harmonics+sag, and (f)harmonics+swell.

depicts the laboratory hardware set up utilized to generate various PQDs. In order to accurately represent the dynamics of real-world PQDs, numerical models for PQDs have been deployed using MATLAB.

A dataset of 330 signals comprising of 11 different classes with 30 signals of each class was subsequently generated using dSPACE DS1104RD Control-Desk. These signals were generated using the DAC output of the DS1104RD board, and recorded with YOKOGAWA DLM2024 Mixed Signal Oscilloscope (MSO). Notably, each signal is recorded for 10 cycles with 125 samples per cycle sampling rate. Fig. 10 represents various PQD waveforms of hardware signals captured using the MSO.

The statistical features have been extracted in a similar way as described in section III. Considering the performance analysis presented in previous sub-sections, it is clear that the performance of LRM, RF, and ET classifiers is better in comparison to the other classifiers with the proposed features. As a result, an evaluation with hardware signals is carried out with LRM, RF, and ET classifiers only. It is noteworthy that all classifiers have been trained on only simulated data and tested with unseen hardware signals. The purpose of this thorough assessment is to confirm the generalized capabilities and robustness of the suggested classification framework. This methodology serves as a strong demonstration of the practical applicability of the proposed approach. Table 5 represents the performance in terms of class-wise accuracy for the classifiers with different mother wavelets.

Compared to the LRM and RF classifiers, the ET classifier performed better with all mother wavelets in classifying hardware PQD signals, as depicted in Table 5. Overall, the ET classifier with the 'haar' mother wavelet demonstrated

TABLE 5. Performance of classifiers with hardware signals.

Wavelet	'db4'			'haar'			'dmey'			'coif4'		
Class	**LRM**	**RF**	**ET**	**LRM**	**RF**	**ET**	**LRM**	**RF**	**ET**	**LRM**	**RF**	**ET**
CL1 (Normal)	83.33%	96.67%	96.67%	80%	100%	100%	76.67%	86.67%	86.67%	60%	83.33%	86.67%
CL2 (Sag)	93.33%	100%	100%	96.67%	100%	100%	93.33%	96.67%	96.67%	100%	100%	100%
CL3 (Swell)	100%	100%	100%	100%	100%	100%	80%	100%	100%	100%	100%	100%
CL4 (Interruption)	100%	86.67%	80%	96.67%	93.33%	96.67%	80%	76.67%	76.67%	100%	90%	93.93%
CL5 (Impulsive Transient)	86.67%	100%	100%	83.33%	100%	100%	66.67%	93.33%	86.67%	56.67%	86.67%	90%
CL6 (Oscillatory Transient)	86.67%	100%	96.67%	96.67%	90%	93.33%	96.67%	100%	96.67%	90.00%	100%	96.67%
CL7 (Harmonics)	96.67%	90%	100%	100%	100%	100%	90%	100%	100%	100.%	100%	100%
CL8 (Flicker)	100%	100%	100%	96.67%	100%	100%	93.33%	100%	100%	96.67%	100%	100%
CL9 (Notches)	100%	93.33%	96.67%	93.33%	100%	100%	83.33%	100%	100%	80%	96.67%	100%
CL10 (Sag with Harmonics)	70%	96.67%	96.67%	100%	83.33%	96.67%	70.00%	86.67%	100%	100%	96.67%	100%
CL11 (Swell with Harmonics)	100%	100%	100%	100%	100%	100%	93.33%	100%	100%	100%	100%	100%
Overall Accuracy	**92.42%**	**96.67%**	**96.97%**	**94.85%**	**96.97%**	**98.79%**	**83.94%**	**94.55%**	**94.85%**	**89.39%**	**95.76%**	**96.97%**

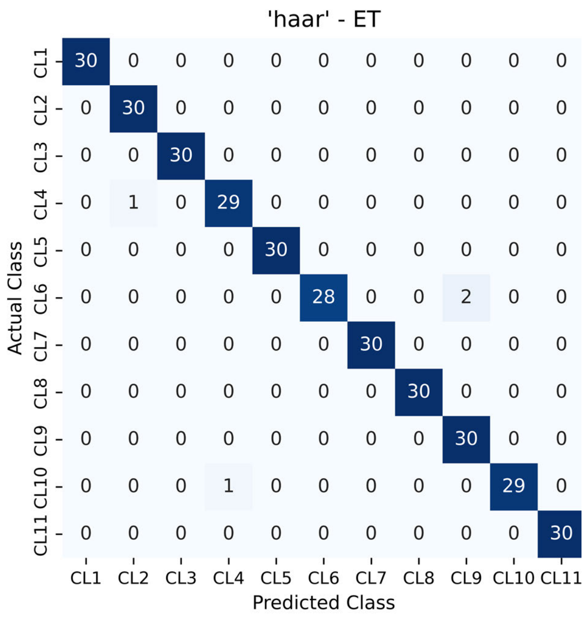

FIGURE 11. Confusion matrix for ET classifier with 'haar' wavelet for hardware signals.

remarkable performance, achieving 98.79% classification accuracy. The confusion matrix for the ET classifier with the 'haar' mother wavelet is shown in Fig. 11. The ET classifier has correctly classified 326 out of total 330 hardware PQD signals which validates the superiority of proposed classification approach.

Furthermore, the performance of the classifiers in terms of precision, recall, and F1 score of testing is tabulated in Table 6 for the 'haar' mother wavelet. The precision, recall, and F1

TABLE 6. Performance parameters of the ET classifiers with 'haar' mother wavelet.

Classifier	F1 Score	Precision	Recall
LRM	94.87%	95.02%	94.85%
RF	96.95%	97.21%	96.97%
ET	98.79%	98.84%	98.79%

values are calculated as per the equations presented in [47]. Higher precision signifies fewer false positives while higher recall indicates fewer false negatives. Moreover, a higher F1 score signifies the ability of classifier to achieve both high precision and high recall.

From Table 6, it is evident that ET classifier has achieved highest precision (98.84%), recall (98.79%) and F1 (98.79%) scores while classifying unseen hardware PQD signals, demonstrating its superior and optimized performance among all the classifiers considered in the present work.

D. PERFORMANCE WITH REAL PQD EVENT SIGNALS

To further assess the effectiveness of the proposed approach, real PQD event signals collected from the electrical grid are used for testing. This dataset comprises real-life PQD events of 26 sag signals and 42 impulsive transient signals available at [43], [44]. In this dataset, the signals having a fundamental frequency of 50 Hz were captured at a sampling frequency of 20 kHz. Prior to the feature extraction using DWT, the real signals are normalized. The extracted features are used to evaluate the performance of the LRM, RF, and ET classifiers trained on synthetic PQD signals. The subsequent results provide a detailed performance comparison. The results obtained are presented in Table 7 in terms of the number of

TABLE 7. Performance of classifiers with real PQD signals.

Mother Wavelet	ML Classifier	Number of Misclassifications	
		Sag (Out of 26)	Impulsive Transient (Out of 42)
db4	LRM	5	11
	RF	4	9
	ET	4	8
haar	LRM	4	8
	RF	3	8
	ET	3	6
dmey	LRM	7	12
	RF	6	11
	ET	6	11
coif4	LRM	7	10
	RF	5	8
	ET	3	8

TABLE 8. Performance comparison with the existing techniques.

Ref	Feature Extraction and Classification	No of Class	Accuracy
[13]	TQWT + DMSVM	14	98.78% (Syn.) 96.42% (20 dB)
[19]	EWT + FFNN	19	98.1% (Syn.) 96.05% (20 dB)
[17]	ST + HT + RBDT	9	99.3% (Syn.)
[14]	WT + ANN	14	98.21% (Syn.)
Proposed	DWT ('haar') + ET	11	99.81% (Syn) 96.18% (20 dB) 98.78% (Har.)

Syn.: Synthetic Signals, Har.: Hardware Signals

misclassification events. The performance of the 'haar-RF' and 'coif4-ET' approaches is identical. Whereas, the 'haar-ET' approach has superior performance in classifying real PQD events.

E. PERFORMANCE COMPARISON WITH EXISTING TECHNIQUES

In this section, the performance of 'haar-ET' based scheme is compared with other existing methods. Table 8 provides a detailed summary of the comparison with other existing methods. The existing techniques have utilized various features and ML algorithms for classifying PQDs as mentioned in Table 8.

The proposed method, which combines the features extracted using DWT with the 'haar' mother wavelet and ET classifier, exhibits superior performance in classifying PQDs with a remarkable 99.81% accuracy for noiseless signals. Moreover, it maintains a high accuracy of 96.18% even in the presence of 20 dB of SNR. Notably, unlike other mentioned methods, noise signals were not part of the training dataset in the proposed work. Furthermore, the performance of many existing techniques has not been evaluated with hardware signals. When tested with 330 unseen hardware PQDs signals, the proposed technique demonstrated reliable performance by accurately classifying 326 signals. Furthermore, the promising performance with real PQD events highlights the applicability of the proposed approach in real-world scenarios. Overall, the performance of the proposed 'haar-ET' based technique is superior to other mentioned existing techniques for classifying PQDs.

V. CONCLUSION

This study conducts feature extraction and classification of PQDs employing six distinct ML algorithms with DWT. The proposed methodology entails the extraction of mixed-order statistical features from PQDs signals utilizing four mother wavelets, namely 'db4', 'haar', 'dmey', and 'coif4'. Evaluation of algorithmic accuracy is performed on synthetic datasets encompassing both noise-free and noisy signals. Additionally, validation of the proposed algorithms is carried out using signals obtained from the experimental setup as well as real PQD signals. The results indicate that the 'haar-ET' based approach consistently outperforms other considered methods, achieving an accuracy of 99.81% on noise-free signals. Furthermore, the adaptability and robustness of the 'haar-ET' method are evidenced by its accuracy of 96.18% on unseen noisy signals with an SNR of 20 dB and 98.78% on hardware signals. Also, the 'haar-ET' based scheme demonstrated accuracy of 88.46% in the classification of real-world sag and impulsive transient signals.

Although the 'haar-ET' methodology has demonstrated superior performance with features considered in this study, it is still important to explore future research directions. Subsequent research endeavors may explore the application of alternative mother wavelets, different feature sets, and emerging ML classifiers to enhance the accuracy of PQD classification. Expanding the dataset to include diverse real-world PQD event scenarios will also help to generalize the findings and improve the robustness of the PQD classification algorithms.

REFERENCES

[1] R. C. Dugan, S. Santoso, M. F. McGranaghan, and H. W. Beaty, "Electrical power systems quality," in *McGraw-Hill Professional Engineering*. New York, NY, USA: McGraw-Hill, 2002.

[2] M. H. J. Bollen and I. Y. Gu, *Signal Processing of Power Quality Disturbances*. Hoboken, NJ, USA: Wiley, 2006, doi: 10.1002/0471931314.

[3] A. A. Alkahtani, S. T. Y. Alfalahi, A. A. Athamneh, A. Q. Al-Shetwi, M. B. Mansor, M. A. Hannan, and V. G. Agelidis, "Power quality in microgrids including supraharmonics: Issues, standards, and mitigations," *IEEE Access*, vol. 8, pp. 127104–127122, 2020, doi: 10.1109/ACCESS.2020.3008042.

[4] Y. Wang, J. Ravishankar, and T. Phung, "Wavelet transform-based feature extraction for detection and classification of disturbances in an islanded micro-grid," *IET Gener., Transmiss. Distribution*, vol. 13, no. 11, pp. 2077–2087, Jun. 2019, doi: 10.1049/iet-gtd.2018.5131.

[5] A. A. Abdelsalam, A. A. Eldesouky, and A. A. Sallam, "Characterization of power quality disturbances using hybrid technique of linear Kalman filter and fuzzy-expert system," *Electric Power Syst. Res.*, vol. 83, no. 1, pp. 41–50, Feb. 2012, doi: 10.1016/j.epsr.2011.09.018.

[6] Y. H. Gu and M. H. J. Bollen, "Time-frequency and time-scale domain analysis of voltage disturbances," *IEEE Trans. Power Del.*, vol. 15, no. 4, pp. 1279–1284, Aug. 2000, doi: 10.1109/61.891515.

[7] P. Khetarpal and M. M. Tripathi, "A critical and comprehensive review on power quality disturbance detection and classification," *Sustain. Computing: Informat. Syst.*, vol. 28, Dec. 2020, Art. no. 100417, doi: 10.1016/j.suscom.2020.100417.

[8] M. Mishra, "Power quality disturbance detection and classification using signal processing and soft computing techniques: A comprehensive review," *Int. Trans. Electr. Energy Syst.*, vol. 29, no. 8, Aug. 2019, Art. no. e12008, doi: 10.1002/2050-7038.12008.

[9] G. S. Chawda, A. G. Shaik, M. Shaik, S. Padmanaban, J. B. Holm-Nielsen, O. P. Mahela, and P. Kaliannan, "Comprehensive review on detection and classification of power quality disturbances in utility grid with renewable energy penetration," *IEEE Access*, vol. 8, pp. 146807–146830, 2020, doi: 10.1109/ACCESS.2020.3014732.

[10] S. Khokhar, A. A. Mohd Zin, A. P. Memon, and A. S. Mokhtar, "A new optimal feature selection algorithm for classification of power quality disturbances using discrete wavelet transform and probabilistic neural network," *Measurement*, vol. 95, pp. 246–259, Jan. 2017, doi: 10.1016/j.measurement.2016.10.013.

[11] S. Santoso, W. M. Grady, E. J. Powers, J. Lamoree, and S. C. Bhatt, "Characterization of distribution power quality events with Fourier and wavelet transforms," *IEEE Trans. Power Del.*, vol. 15, no. 1, pp. 247–254, Aug. 2000, doi: 10.1109/61.847259.

[12] K. Manimala, K. Selvi, and R. Ahila, "Optimization techniques for improving power quality data mining using wavelet packet based support vector machine," *Neurocomputing*, vol. 77, no. 1, pp. 36–47, Feb. 2012, doi: 10.1016/j.neucom.2011.08.010.

[13] K. Thirumala, M. S. Prasad, T. Jain, and A. C. Umarikar, "Tunable-Q wavelet transform and dual multiclass SVM for online automatic detection of power quality disturbances," *IEEE Trans. Smart Grid*, vol. 9, no. 4, pp. 3018–3028, Jul. 2018, doi: 10.1109/TSG.2016.2624313.

[14] L. C. M. de Andrade, T. Nanjundaswamy, M. Oleskovicz, R. A. S. Fernandes, and K. Rose, "Advances in classification and compression of power quality signals," *J. Control, Autom. Electr. Syst.*, vol. 30, no. 3, pp. 402–412, Jun. 2019, doi: 10.1007/s40313-019-00446-1.

[15] S. Naderian and A. Salemnia, "Method for classification of PQ events based on discrete Gabor transform with FIR window and T2FK-based SVM and its experimental verification," *IET Gener., Transmiss. Distrib.*, vol. 11, no. 1, pp. 133–141, Jan. 2017, doi: 10.1049/iet-gtd.2016.0703.

[16] S. Chen, Z. Li, G. Pan, and F. Xu, "Power quality disturbance recognition using empirical wavelet transform and feature selection," *Electronics*, vol. 11, no. 2, p. 174, Jan. 2022, doi: 10.3390/electronics11020174.

[17] N. Kumar Swarnkar, O. Prakash Mahela, B. Khan, and M. Lalwani, "Identification and classification of multiple power quality disturbances using a parallel algorithm and decision rules," *Energy Eng.*, vol. 119, no. 2, pp. 473–497, 2022, doi: 10.32604/ee.2022.017703.

[18] H. Erişti, Ö. Yıldırım, B. Erişti, and Y. Demir, "Optimal feature selection for classification of the power quality events using wavelet transform and least squares support vector machines," *Int. J. Electr. Power Energy Syst.*, vol. 49, pp. 95–103, Jul. 2013, doi: 10.1016/j.ijepes.2012.12.018.

[19] K. Thirumala, A. Kanjolia, T. Jain, and A. C. Umarikar, "Empirical wavelet transform and dual feed-forward neural network for classification of power quality disturbances," *Int. J. Power Energy Convers.*, vol. 11, no. 1, p. 1, 2020, doi: 10.1504/ijpec.2020.104805.

[20] H. Sindi, M. Nour, M. Rawa, Ş. Öztürk, and K. Polat, "A novel hybrid deep learning approach including combination of 1D power signals and 2D signal images for power quality disturbance classification," *Exp. Syst. Appl.*, vol. 174, Jul. 2021, Art. no. 114785, doi: 10.1016/j.eswa.2021.114785.

[21] N. M. Rodrigues, F. M. Janeiro, and P. M. Ramos, "Deep learning for power quality event detection and classification based on measured grid data," *IEEE Trans. Instrum. Meas.*, vol. 72, pp. 1–11, 2023, doi: 10.1109/TIM.2023.3293555.

[22] Y. Liu, D. Yuan, H. Fan, T. Jin, and M. A. Mohamed, "A multidimensional feature-driven ensemble model for accurate classification of complex power quality disturbance," *IEEE Trans. Instrum. Meas.*, vol. 72, pp. 1–13, 2023, doi: 10.1109/TIM.2023.3265756.

[23] Y. Deng, H. Jia, P. Li, X. Tong, and F. Li, "A deep learning method based on long short term memory and sliding time window for type recognition and time location of power quality disturbance," in *Proc. Chinese Autom. Congr. (CAC)*, 2019, vol. 15, no. 8, pp. 1764–1768, doi: 10.1109/CAC.2018.8623810.

[24] X. Wang, G.-H. Bi, S.-L. Chen, and Z. Zu, "A method to analyze power system quality disturbing signal based on recurrence quantification analysis," *Proc. Eng.*, vol. 15, pp. 4115–4121, 2011, doi: 10.1016/j.proeng.2011.08.772.

[25] D. Moyal, N. Kothari, P. Vaghera, and D. Kumar, "Classifying power quality disturbance using time and multiresolution features through artificial neural network," in *Proc. Int. Conf. Intell. Technol. (CONIT)*, Jun. 2021, pp. 1–5, doi: 10.1109/CONIT51480.2021.9498515.

[26] P. Vaghera, D. Kumar, N. Kothari, and S. Niamatullah, "Identification of the source of power quality degradation using signature extraction from voltage waveforms," in *Proc. Adv. Electr. Power Energy Infrastruct.*, 2020, pp. 219–227, doi: 10.1007/978-981-15-0206-4_19.

[27] I. Parvez, M. Aghili, A. I. Sarwat, S. Rahman, and F. Alam, "Online power quality disturbance detection by support vector machine in smart meter," *J. Modern Power Syst. Clean Energy*, vol. 7, no. 5, pp. 1328–1339, Sep. 2019, doi: 10.1007/s40565-018-0488-z.

[28] G. T. Heydt and A. W. Galli, "Transient power quality problems analyzed using wavelets," *IEEE Trans. Power Del.*, vol. 12, no. 2, pp. 908–915, Apr. 1997, doi: 10.1109/61.584412.

[29] I. Daubechies, *Ten Lectures on Wavelets*. Philadelphia, PA, USA: Society for Industrial and Applied Mathematics, 1992, doi: 10.1137/1.9781611970104.

[30] S. G. Mallat, "A theory for multiresolution signal decomposition: The wavelet representation," *IEEE Trans. Pattern Anal. Mach. Intell.*, vol. 11, no. 7, pp. 674–693, Jul. 1989, doi: 10.1109/34.192463.

[31] G. Guo, H. Wang, D. Bell, Y. Bi, and K. Greer, "KNN model-based approach in classification," in *On The Move to Meaningful Internet Systems 2003: CoopIS, DOA, and ODBASE*, R. Meersman, Z. Tari, and D. C. Schmidt, Eds., Berlin, Germany: Springer, 2003, pp. 986–996, doi: 10.1007/978-3-540-39964-3_62.

[32] I. H. Sarker, "Machine learning: Algorithms, real-world applications and research directions," *Social Netw. Comput. Sci.*, vol. 2, no. 3, p. 160, May 2021, doi: 10.1007/s42979-021-00592-x.

[33] S. L. David and W. Hosmer, "Introduction to the logistic regression model," in *Applied Logistic Regression*. Hoboken, NJ, USA: Wiley, 2000, pp. 1–30, doi: 10.1002/0471722146.ch1.

[34] E. Makalic and D. F. Schmidt, "Review of modern logistic regression methods with application to small and medium sample size problems," in *AI 2010: Advances in Artificial Intelligence*, J. Li, Ed., Berlin, Germany: Springer, 2010, pp. 213–222, doi: 10.1007/978-3-642-17432-2_22.

[35] L. Rokach and O. Maimon, "Decision trees," in *Data Mining and Knowledge Discovery Handbook*, O. Maimon and L. Rokach, Eds., Boston, MA, USA: Springer, 2005, pp. 165–192, doi: 10.1007/0-387-25465-X_9.

[36] C. M. Bishop and N. M. Nasrabadi, *Pattern Recognition and Machine Learning*, vol. 4, no. 4. New York, NY, USA: Springer, 2006.

[37] L. Breiman, "Random forests," *Mach. Learn.*, vol. 45, no. 1, pp. 5–32, 2001, doi: 10.1023/A:1010933404324.

[38] P. Geurts, D. Ernst, and L. Wehenkel, "Extremely randomized trees," *Mach. Learn.*, vol. 63, no. 1, pp. 3–42, Apr. 2006, doi: 10.1007/s10994-006-6226-1.

[39] R. Machlev, A. Chachkes, J. Belikov, Y. Beck, and Y. Levron, "Open source dataset generator for power quality disturbances with deep-learning reference classifiers," *Electric Power Syst. Res.*, vol. 195, Jun. 2021, Art. no. 107152, doi: 10.1016/j.epsr.2021.107152.

[40] *IEEE Recommended Practice for Monitoring Electric Power Quality*, IEEE Standard 1159-2019, 2019, pp. 1–98, doi: 10.1109/IEEESTD.2019.8796486.

[41] U. Sipai, R. Jadeja, N. Kothari, and T. Trivedi, "Synthetic power quality disturbances dataset of single and combined disturbances generated in accordance with IEEE 1159 specifications," *IEEE Dataport*, Feb. 2024, doi: 10.21227/035e-rx20.

[42] U. Sipai, R. Jadeja, N. Kothari, and T. Trivedi, "Power quality disturbances dataset of single and combined disturbances," *Harvard Dataverse*, 2024, doi: 10.7910/DVN/PC44W4.

[43] O. Florencias-Oliveros, M. J. Espinosa-Gavira, J.-J. G. de la Rosa, A. Agüera-Pérez, J. C. Palomares-Salas, and J. M. Sierra-Fernández, "Real-life power quality sags," *IEEE Dataport*, May 2017, doi: 10.21227/H2K88D.

[44] O. Florencias-Oliveros, M. J. Espinosa-Gavira, J. J. González-de-la-Rosa, A. Agüera-Pérez, J. C. P. Salas, and J. M. Sierra-Fernández, "Real-life power quality transients," *IEEE Dataport*, May 2017, doi: 10.21227/H2Q30W.

[45] J. Barros, R. I. Diego, and M. de Apráiz, "Applications of wavelets in electric power quality: Voltage events," *Electric Power Syst. Res.*, vol. 88, pp. 130–136, Jul. 2012, doi: 10.1016/j.epsr.2012.02.009.

[46] G. Hinton and S. Roweis, "Stochastic neighbor embedding," in *Proc. 15th Int. Conf. Neural Inf. Process. Syst.*, 2002, pp. 833–840, doi: 10.1007/978-3-031-10602-6_16.
[47] M. Grandini, E. Bagli, and G. Visani, "Metrics for multi-class classification: An overview," 2020, *arXiv:2008.05756*.

UVESH SIPAI (Member, IEEE) received the B.E. degree in electrical engineering from Gujarat Technological University, Rajkot, India, in 2014, and the M.Tech. degree in power electronics and electrical machines drives from Nirma University, Ahmedabad, India, in 2016. He is currently pursuing the Ph.D. degree in electrical engineering with Marwadi University, Rajkot.

From 2015 to 2016, he was a Teaching Assistant with Nirma University. Since 2016, he has been an Assistant Professor of electrical engineering with Marwadi University. He has made significant contributions to the academic and research community, having published four conference papers and 22 intellectual property rights (IPR), including copyrights, industrial designs, and patents. His research interests include power quality, application of AI in electrical engineering, renewable energy conversion systems, and multi-level inverters.

Prof. Sipai is an Active Member of the IEEE Industrial Application Society, the IEEE Industrial Electronics Society, and the IEEE Power and Energy Society. He achieved academic distinction, securing the Gold Medal for excellence during the M.Tech. degree at Nirma University, in 2016, and he earned an International Scholarship Exchange for the Ph.D. Candidates at Lodz University of Technology, Poland, in 2019, through the esteemed PROM Project by NAWA and European Social Fund.

RAJENDRASINH JADEJA (Senior Member, IEEE) received the B.E. degree in electrical engineering from the L.D. College of Engineering, Gujarat University, in 1998, the M.Tech. degree in electrical engineering from Nirma University, and the Ph.D. degree from The Maharaja Sayajirao University of Baroda. He is currently the Pro-Vice-Chancellor of Marwadi University, India. He is also a Postdoctoral Fellow (PDF) with Jan Wyzykowski University, Polkowice, Poland. He has undertaken and completed a project funded by Gujarat Council on Science and Technology (GUJCOST) and is involved on a project making deep learning and AI skills mainstream in India to fulfill trilateral needs of entrepreneurship, industry-academia partnership, and application-inspired engineering research. He actively participates and initiates ERASMUS+ for staff mobility and completed such a program for teaching between partner countries. His research interests include control of power electronic converters, AC drives, pulse width modulated power electronic converters, and power quality issues and their mitigation techniques. He has been awarded the title ING.PAED.IGIP, in 2020. He was a Treasurer of the IEEE India Council from 2019 to 2020 and the Chair of the IEEE Gujarat Section from 2017 to 2018. He was a Treasurer of IEEE R-10 from 2021 to 2022 and the Chair of the IEEE R10 Membership Development Committee from 2022 to 2023. He is also serving as the Vice Chair for the IEEE R10 Membership Activities Committee.

NISHANT KOTHARI (Member, IEEE) received the M.E. degree from The Maharaja Sayajirao University of Baroda, and the Ph.D. degree from RK University, Rajkot. He is currently an Associate Professor with the Department of Electrical Engineering, Marwadi University, India. He has published 11 articles and seven intellectual property rights (IPR), including copyrights and design patents. His research interests include power system protection, application of artificial intelligence to power systems, electrical machines, and power quality analysis. He received two best paper awards at reputed international conferences.

TAPANKUMAR TRIVEDI (Senior Member, IEEE) received the M.Tech. degree from Indian Institute of Technology (IIT) at Roorkee, Roorkee, and the Ph.D. degree from the Charotar University of Science and Technology.

He is currently an Associate Professor with the Department of Electrical Engineering, Marwadi University, India. His research interests include power quality improvement devices, control of power electronic converters, and multiphase drives.

Dr. Trivedi received research grants for projects Evaluation of Current Control Strategy and Direct Power Control Algorithm for Shunt Active Power Filter and Rescue Support Robotics for Earthquake Situations from Gujarat Council on Science and Technology (GUJCOST), Government of Gujarat. He is a reviewer of various reputed journals, including IEEE TRANSACTIONS ON INDUSTRY APPLICATIONS and *IET Power Electronics*.

RAJESH MAHADEVA (Member, IEEE) received the B.E. degree in electronics and instrumentation engineering from the Samrat Ashok Technological Institute (SATI), Vidisha, Madhya Pradesh, India, in 2006, the M.Tech. degree in control and instrumentation engineering from the National Institute of Technology (NIT), Jalandhar, Punjab, India, in 2009, and the Ph.D. degree from the Department of Polymer and Process Engineering, Indian Institute of Technology (IIT) at Roorkee, Roorkee, Uttarakhand, India, in 2022. From 2011 to 2017, he was an Assistant Professor with the Technocrats Institute of Technology (TIT), Bhopal, and Marwadi University (MU), Rajkot, India. He is currently a Research Scientist with the Department of Physics, Khalifa University, Abu Dhabi, United Arab Emirates. His research interests include modeling, simulation, optimization, and control of desalination and water treatment plants/processes using artificial intelligence techniques.

SHASHIKANT P. PATOLE (Member, IEEE) received the B.Sc., M.Sc., and M.Phil. degrees in physics from the University of Pune (UoP), India, and the Ph.D. degree in nanoscience and technology from Sungkyunkwan University (SKKU), Suwon, South Korea, in 2010. Since 2017, he has been an Assistant Professor with the Physics Department, Khalifa University (KU), Abu Dhabi, United Arab Emirates. Before joining KU, he was an Entrepreneur and a Postdoctoral Researcher with the King Abdullah University of Science and Technology (KAUST), Saudi Arabia. In KAUST, he was the Founding Member of the Laboratory for Carbon Nanostructures and the Co-Founder of a Graphene Crystal Startup Company. He has published more than 50 articles. His research interests include the development and commercialization of advanced quantum materials for sustainable energy and environment carbon nanotubes, graphene, and other 2-D materials in membrane technology, structural composites and energy, optoelectronics, electron field emission, and photovoltaic, and aberration-corrected transmission electron microscopy.